THERMOELECTRIC PROPERTIES OPTIMIZATION OF PEDOT:PSS FOR ORGANIC THERMOELECTRIC GENERATOR

A Thesis

Presented to the Faculty of the Graduate School

of Cornell University

in Partial Fulfillment of the Requirements for the Degree of

Master of Science

by

Liwei Shi

August 2023

ABSTRACT

The thermoelectric effect, otherwise known as "Seebeck effect", is the direct conversion of a temperature difference between two dissimilar electrical conductors or semiconductors to an electrical voltage. By making use of this process, the thermoelectric generator (TEG) becomes a promising technology for the waste heat recovery. Compared to other energy-harvesting technologies, TEG exhibits distinct advantages such as it can be used remotely, can operate in silence and no gaseous or chemical waste is produced during operation. An ordinary TEG contains multiple couples of one p-type and one n-type thermoelectric unit. Therefore in order to build a TEG, choosing thermoelectric (TE) materials either inorganic or organic becomes the top priority. As the most common inorganic TE material, PEDOT:PSS has received an extensive scientific interest in recent years. This review covers the motivation of developing organic thermoelectric generators (OTEG), techniques for PEDOT:PSS material preparation, material properties' measurement and analysis, and the thermoelectric performance optimization process. Finally, some challenges and future expectations are provided for further levels of development.

BIOGRAPHICAL SKETCH

The author of this thesis, Liwei Shi, was born on Nov.26th in 1998 in Ningbo. Growing up in Ningbo, China. He developed a keen interest in engineering from a young age. This early fascination with engineering shaped his educational journey and ultimately led to the completion of this research. Liwei Shi pursued his undergraduate studies at Case Western University, where he obtained a Bachelor's degree in Mechanical Engineering with honors. During his undergraduate years, he actively engaged in various extracurricular activities, such as engineering student association and robot design competition which allowed him to enhance his leadership skills and develop a well-rounded perspective. Motivated by his passion for Mechanical Engineering, Liwei decided to pursue advanced studies in Mechanical Engineering at Cornell University. He was admitted into the Master of Science program and joined the ZT group under Professor Tian, where he delved deeper into the intricacies of mechanical design and thermal science. The rigorous coursework and research opportunities provided him with a solid foundation in this field, equipping him with the necessary tools to undertake this thesis. With this thesis, Liwei aims to contribute to the existing body of knowledge in Mechanical Engineering and address the research gap surrounding organic thermoelectric generator. His dedication, passion, and commitment to excellence have driven them to conduct meticulous research, analyze data, and present well-supported conclusions. It is his hope that this thesis will provide valuable insights and inspire further exploration in this field.

This document is dedicated to all Cornell graduate students.

ACKNOWLEDGEMENTS

I would like to express my deepest gratitude and appreciation to all those who have supported me throughout the process of completing this thesis. First and foremost, I am immensely grateful to my thesis advisor, Professor Zhiting Tian, for her invaluable guidance, expertise, and unwavering support. Her insightful feedback, constructive criticism, and dedication have been instrumental in shaping the direction and quality of this research. I am also thankful to the second member of my thesis committee, Professor Yoo L. Joo, for his time, expertise, and valuable input. His thoughtful suggestions and constructive discussions have greatly contributed to the refinement of this thesis. I extend my heartfelt appreciation to the lab mates and researchers in the ZT Group for creating a stimulating academic environment. Their commitment to excellence and their willingness to share their knowledge and expertise have been crucial in my intellectual growth. Additionally, I am indebted to the staff and personnel at Cornell University for their administrative support and assistance throughout my studies. Their efficiency and professionalism have greatly facilitated the completion of this thesis. Last but not least, I would like to express my gratitude to my family and friends for their unwavering love, encouragement, and understanding. Their constant support, belief in my abilities, and patience during challenging times have been a constant source of motivation. In conclusion, this thesis would not have been possible without the collective support and encouragement of all those mentioned above, as well as many others who have contributed to my growth as a researcher. I am truly grateful for their unwavering support and belief in my abilities.

TABLE OF CONTENTS

LIST OF TABLES

LIST OF FIGURES

CHAPTER 1

INTRODUCTION

This introductory chapter first gives an overview of the background and describes the motivation for this thesis. Subsequently, the research objectives are formulated, and this chapter finishes with a thesis outline stating the further structure.

1.1 Background

In recent years, the demand for sustainable and efficient energy harvesting technologies has become increasingly vital in addressing the global energy crisis and mitigating the impact of climate change. Among the various emerging technologies, organic thermoelectric generators (OTEGs) have attracted significant attention due to their potential to convert waste heat into usable electrical energy [1,2]. One promising material for OTEGs is poly(3,4-ethylenedioxythiophene):poly(styrenesulfonate) (PEDOT:PSS), a conductive polymer known for its favorable thermoelectric properties and compatibility with low-cost fabrication processes [3,4].

The thermoelectric properties of PEDOT:PSS, including its electrical conductivity, Seebeck coefficient, and thermal conductivity, play crucial roles in determining the efficiency of OTEGs. Enhancing these properties is essential for improving the overall performance of PEDOT:PSS-based devices [4,5]. Electrical conductivity is a key factor affecting the charge carrier transport in the material, while the Seebeck coefficient reflects its ability to convert a thermal gradient

into an electrical voltage. Additionally, thermal conductivity directly impacts the heat dissipation within the device and influences its efficiency in converting heat into electricity [3,4].

1.2 Motivation

Organic thermoelectric generators (OTEGs) have garnered significant attention in recent years due to their distinct advantages over traditional inorganic thermoelectric generators. OTEGs offer remarkable flexibility and lightweight characteristics, enabling their integration into unconventional shapes and structures [6]. These properties make OTEGs particularly appealing for applications in wearable electronics, curved surfaces, and conformal energy harvesters [3].

Additionally, OTEGs benefit from compatibility with low-cost and scalable fabrication techniques [7]. Solution processing of organic materials, such as PEDOT:PSS, allows for cost-effective large-scale production, opening up possibilities for widespread adoption and integration into energy harvesting systems [4].

Another appealing feature of OTEGs is their inherently lower thermal conductivities compared to inorganic materials [5]. This property minimizes heat dissipation within the device, enhancing the overall thermoelectric efficiency in converting heat energy into electrical energy.

In summary, the combination of flexibility, low-cost fabrication compatibility, and lower thermal conductivities positions OTEGs as a promising field of research and motivates researchers to explore more in this field. By harness-

ing waste heat and converting it into usable electrical energy using lightweight, flexible, and cost-effective devices, OTEGs have the potential to significantly contribute to energy sustainability and efficiency.

1.3 Research Objectives

This master's thesis aims to explore the optimization of the thermoelectric properties of PEDOT:PSS for OTEGs. By investigating the key factors influencing the thermoelectric performance of this material and developing strategies to enhance its efficiency, this study seeks to contribute to the advancement of OTEG technology.

The research objectives can be divided into two key components. Firstly, the fundamental principles governing the thermoelectric behavior of PEDOT:PSS will be analyzed to identify the critical parameters affecting its performance. This analysis will involve building the measurement device, fabricating film samples, and investigating the impact of various factors such as surface morphology, film thickness and molecular structure on the thermoelectric properties of PEDOT:PSS.

Secondly, various techniques and strategies will be proposed and evaluated to optimize these properties through material engineering and process optimization. This includes exploring novel doping approaches, post-treatment, and optimizing the film morphology to enhance the thermoelectric performance of PEDOT:PSS. Additionally, process parameters such as the selection of solvents, solution concentration, and treatment time will be investigated to maximize the thermoelectric efficiency of PEDOT:PSS films.

1.4 Thesis Outline

To achieve these objectives, the thesis will follow a structured approach. Chapter 3 involves a comprehensive literature review on PEDOT:PSS and thermoelectric materials, providing a solid foundation for understanding the underlying mechanisms of thermoelectricity and the current state of research in the field.

Chapter 4 outlines the experimental approaches, addressing both two key components of research objectives which include the design and establishment of thermoelectric properties measuring device, the fabrication of PEDOT:PSS film samples, and the optimization process. All the details will be presented in this chapter and the empirical analysis will contribute to bridging the gap between theoretical understanding and practical application.

Chapter 5 presents the findings obtained from the experimental investigations. It includes the characterization of the thermoelectric properties of the PEDOT:PSS films, such as film thickness, electrical conductivity and Seebeck coefficient. The performance will also be evaluated and compared. The data collected and analyzed in this chapter will provide insights into the effectiveness of the proposed optimization strategies and the overall thermoelectric efficiency achieved.

Finally, Chapter 6 interprets and analyzes the results in the context of the research objectives and the existing literature. It explores the implications of the findings, identifies trends, and discusses the factors influencing the thermoelectric performance of PEDOT:PSS. The discussion also evaluates the effectiveness of the optimization strategies employed and provides insights into further im-

provements and future directions for research. The limitations of the study will be acknowledged, and recommendations for future work will be proposed.

CHAPTER 2

LITERATURE REVIEW

This thesis mainly analyzes a thermoelectric material, PEDOT:PSS. And this chapter will provide a solid foundation for understanding different types of thermoelectric generators and materials.

Thermoelectric materials have garnered significant interest due to their potential for converting waste heat into usable electrical energy. They find applications in various fields such as power generation, waste heat recovery, and thermal management [8,9]. The thermoelectric performance of a material is typically evaluated using the figure of merit (ZT), which is a measure of the material's ability to simultaneously exhibit high electrical conductivity, a large Seebeck coefficient, and low thermal conductivity [10].

Inorganic thermoelectric materials, such as bismuth telluride (Bi2Te3) and lead telluride (PbTe), have been extensively studied and employed in commercial thermoelectric devices [11,12]. These materials exhibit high electrical conductivities, large Seebeck coefficients, and relatively low thermal conductivities [13]. However, they often suffer from high material and processing costs, limited operating temperature ranges, and environmental concerns associated with the use of toxic elements. Organic thermoelectric materials, including conducting polymers like PEDOT:PSS, have emerged as promising alternatives to inorganic materials [4]. These materials offer advantages such as low-cost fabrication, solution processability, mechanical flexibility, and tunability of electrical and thermal properties through chemical modification and doping [7].

Comparative Analysis of Inorganic and Organic Thermoelectric Materials A

comparative analysis between inorganic and organic thermoelectric materials reveals their distinct advantages and limitations. Inorganic materials excel in terms of high ZT values at elevated temperatures but suffer from cost and processing limitations [13]. Organic materials, on the other hand, offer flexibility, low-cost fabrication, and tunability, but often exhibit lower ZT values at room temperature.

Enhancement Strategies for PEDOT:PSS and Organic Thermoelectric Materials Various strategies have been employed to enhance the thermoelectric performance of PEDOT:PSS and other organic thermoelectric materials [10]. Doping techniques, such as chemical and electrochemical doping, have been utilized to improve electrical conductivity and Seebeck coefficient [3]. Morphology control through solution processing parameters, such as solvent choice and annealing conditions, has been explored to optimize charge transport and reduce thermal conductivity [7]. Furthermore, the incorporation of nanoscale fillers and hybrid composites has shown promise in enhancing the overall thermoelectric properties by balancing electrical and thermal transport [14].

Despite the progress in the field of thermoelectric materials, several challenges remain. The optimization of electrical conductivity, Seebeck coefficient, and thermal conductivity in organic materials is still an ongoing area of research. Additionally, long-term stability, scalability, and device integration of organic thermoelectric materials need further investigation. Future directions include the exploration of novel organic materials, hybrid systems, and advanced manufacturing techniques to improve the overall thermoelectric performance and expand the application potential of organic thermoelectric generators [15].

CHAPTER 3

METHODOLOGY

The methodology chapter explains the research methods and design that were used to conduct the study. The critical parts in this chapter include the design and establishment of thermoelectric properties measuring devices, the fabrication of PEDOT:PSS film samples, and the optimization process.

3.1 Setting

The research study was conducted in the lab of the ZT group at the Sibley School of Mechanical and Aerospace Engineering (MAE) at Cornell University (Fig.1). The Sibley School of MAE is situated within the College of Engineering on the main campus of Cornell University. The campus is located in the picturesque town of Ithaca, surrounded by scenic natural landscapes and offering a vibrant academic atmosphere. The main part of Sibley School is housed in the Upson Hall building, which provides state-of-the-art research facilities and resources for engineering studies.

Some data measurement and analysis processes took place in the Cornell Center for Materials Research (CCMR) at Clark Hall (Fig.2). It is an interdisciplinary research center at Cornell University in Ithaca, New York. CCMR focuses on advancing materials science and engineering through collaborative research, state-of-the-art facilities, and interdisciplinary interactions. With a diverse range of materials research, CCMR aims to address societal challenges, drive technological advancements, and promote innovation. Through its re-

(a) Upson Hall

(b) ZT Group's lab

Figure 1: Sibley School of Mechanical and Aerospace Engineering

search, education, and outreach efforts, CCMR plays a vital role in fostering interdisciplinary collaboration, knowledge exchange, and the development of new materials with enhanced properties and functionalities.

Figure 2: CCMR at Clark Hall

The research was carried out over three consecutive semesters, commencing in Spring 2022 and concluding in Fall 2023. This time frame was chosen according to the 2-year Master of Science program at Cornell University which allows for comprehensive data collection and analysis, ensuring a thorough investigation of the research problem. The study encompassed an extended period to ac-

count for potential variations and fluctuations in experimental conditions, and to facilitate multiple iterations of data collection and analysis. The choice of a multi-semester duration enabled the research team to account for seasonal variations and academic schedules, as well as to provide sufficient time for the implementation of the proposed methodology. The extended time frame allowed for iterative refinement of the research approach and ensured the collection of a robust dataset.

By conducting the research at the Sibley School of MAE within Cornell University and spanning three semesters, the study aimed to leverage the unique resources and expertise available, ensuring a rigorous investigation of the research problem and facilitating comprehensive data collection and analysis.

3.2 Participants

All the participants related to my research are within the ZT Group and we're working on building the organic thermoelectric generator for converting waste heat into electricity together. This project is a part of a larger project supported by the U.S. Department of Energy for upgrading Biogas through in situ Conversion of Carbon Dioxide to Biomethane in Anaerobic Digesters. There're total of five participants currently or have worked on this project, Kevin Kong, a Ms student in Mechanical Engineering who has graduated; Zara Aamer, a Meng student in Mechanical Engineering who has graduated; Samuel Kielar, a PhD student in Material Science Engineering who is still in the group; Sooyon Chang, a Ms student in Mechanical Engineering who is still in the group; and I. We're selected for this project by our common advisor, Professor Zhiting Tian,

by analyzing our preferences and abilities, and Each participant has put a lot of effort into their respective parts. It can be said that without the great help of the mentor and the great efforts of these participants, I couldn't have all the research data, and there would be no this thesis.

3.3 Measurement Instruments

To evaluate a candidate organic or inorganic material's thermoelectric potential in a TEG, the dimensionless ZT figure of merit is used for characterization and comparison,higher the better. And it is defined in (Eq.1).

$$ZT = \frac{\sigma S^2 T}{\lambda} \tag{1}$$

Where σ is the electrical conductivity, S is the Seebeck coefficient, T is the environmental temperature, and λ is the thermal conductivity. However, due to the difficulties in thermal conductivity measurement, researchers usually compare different materials thermoelectric performance by comparing the Power Factor (PF) (Eq.2)

$$PF = \sigma S^2 \tag{2}$$

This research also mainly focuses on optimizing the Power Factor of the samples which means The most basic measuring instrument needs to be able to measure both electrical conductivity and Seebeck coefficient.

3.3.1 Method for Electrical Conductivity Measurement

The electrical conductivity σ plays a crucial role in characterizing the electrical properties of the materials under investigation. It is a fundamental property

that characterizes a material's ability to carry electric current, while resistivity ρ quantifies its resistance to the flow of electricity [16]. The relationship between conductivity and resistivity is given by (Eq.3), where σ equals the reciprocal of ρ.

$$\sigma = \frac{1}{\rho} \tag{3}$$

In practical terms, the measurement of resistivity involves passing an electric current through opposing and parallel faces of a bulk sample and recording the resulting resistance using a four-terminal ohmmeter. Pouillet's Law, represented by (Eq.4), allows us to convert the resistance measurement into the intensive resistivity value by considering the distance between the probes and the cross-sectional area through which the current flows [17].

$$R = \frac{\rho l}{A} \tag{4}$$

where R is the resistance, l is the distance and A is the cross-section area. Although this method adequately determines conductivity in simple wires and polycrystalline bulk materials, it poses challenges when applied to low-dimensional thermoelectric materials. These materials, particularly organic thermoelectric ones with intricate and disordered molecular structures, demand a more rigorous approach to achieve accurate results [18]. Moreover, precise measurements can be compromised in the case of single crystals and small-sized thermoelectric samples due to their expected low resistance values.

The four-probe method, also known as the four-point probe technique, is a reliable method for measuring electrical resistivity and can be applied to both bulk and film samples (Fig.3). It offers distinct advantages over traditional two-probe measurements by eliminating contact resistance and accurately assessing the resistivity of conductive or semi-conductive materials [17].

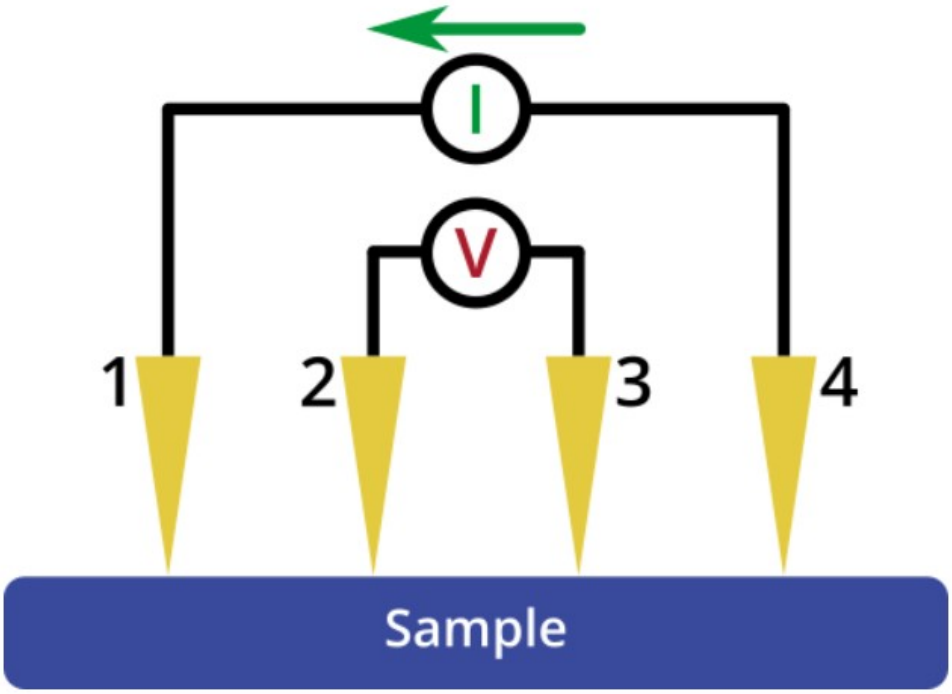

Figure 3: A schematic diagram of four-probe method

In the four-probe method, four evenly spaced probes are positioned on the surface of the sample under test. Two outer probes(1 and 4) inject a known current into the material, while the other two inner probes(2 and 3) measure the resulting voltage drop across a specific distance [19]. The distance between measurement probes must be equal for the four probes for proper measurement. The electrical resistivity is determined by utilizing the current (I) and voltage (V) measurements, taking into account the sample thickness (t) in relation to the probe spacing (s).

For bulk samples with $t >> s$, the resistivity can be calculated from (Eq.5) [20].

$$\rho = 2\pi s(\frac{V}{I}) \tag{5}$$

And for film samples with $t << s$, the resistivity can be calculated from (Eq.6) [20].

$$\rho = \frac{\pi t}{ln2}(\frac{V}{I}) \tag{6}$$

3.3.2 Method for Seebeck Coefficient Measurement

The Seebeck coefficient is a crucial parameter that characterizes the thermoelectric properties of a material. It quantifies the magnitude of the thermoelectric effect, which is the generation of an electric voltage when there is a temperature gradient across a material. The Seebeck coefficient, often denoted as S, represents the ratio of the induced voltage to the temperature difference [21]. To measure the Seebeck coefficient, a common approach is the differential temperature method. This method involves creating a temperature gradient across a sample of the material and measuring the corresponding voltage generated. A temperature gradient is established by heating one end of the sample while keeping the other end at a lower temperature, creating a temperature difference (ΔT) along the sample. By connecting a voltmeter to the sample ends, the induced voltage (ΔV) resulting from the temperature gradient can be measured (Eq.7).

$$S = \pm\frac{\Delta V}{\Delta T} \tag{7}$$

In terms of the sign, the positive charge carrier diffusion prevailing in a p-type material would result in a positive Seebeck coefficient, whereas for n-type thermoelectrics, it would yield a negative value instead [21].

There are various setups for measuring the Seebeck coefficient. A traditional one designed for bulk samples is shown in (Fig.4) below. The material sample

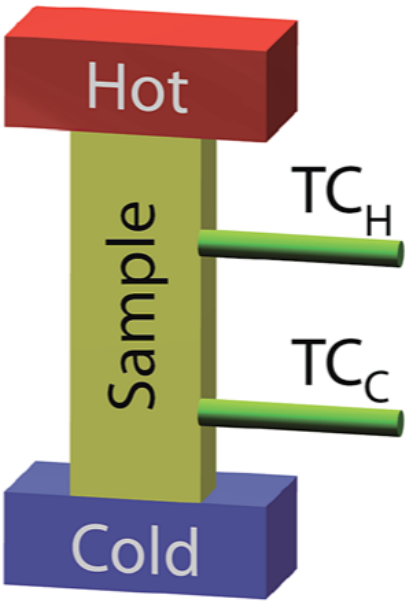

Figure 4: A setup for Seebeck coefficient measurement on bulk samples

is sandwiched between two copper blocks, one works as a heat source and the other works as a heat sink. Therefore the temperature gradient is created across the sample and can be measured by two thermocouples (TC_H and TC_C). And the voltage difference can also be measured at the same two points on the sample by voltmeter.

However, this setup only works for bulk samples. Vertical mounting of film samples is not feasible due to their exceedingly low thickness. In addition, film samples are often grown on substrates that can influence the measured properties, necessitating careful consideration when employing the aforementioned methodology [22]. Taking all these into consideration, novel setups for measuring film samples' Seebeck coefficients, mostly organic thermoelectric materials, are like bridge shapes (Fig.5). Samples are being placed flatly on the copper blocks with some securing methods.

Figure 5: A setup for Seebeck coefficient measurement on film samples

3.3.3 Apparatus Design

In terms of using four-probe method to measure samples' electrical conductivity, a sourecemeter and a voltmeter are essential. Hence KEITHLEY 2450 Sourcemeter and KEITHLEY 2110 Multimeter were ordered through online shop (Fig.6).

(a) KEITHLEY 2450 Sourcemeter (b) KEITHLEY 2110 Multimeter

Figure 6: KEITHLEY Instruments

There are two wires tied to two metal blocks and connected with The positive and negative metal clips of KEITHLEY sourcemeter. These two wires work as the two outer probes in the four-probe method, which are used to source and

record the constant current supply to the sample. As for the inner two probes, we directly used the probes from KEITHLEY multimeter and measured the voltage by our hands. (Fig.7) shows the apparatus configuration used to measure a PEDOT:PSS film sample, excluding the two inner probes from the multimeter. All four probes are quite flexible and can be applied to different location on the

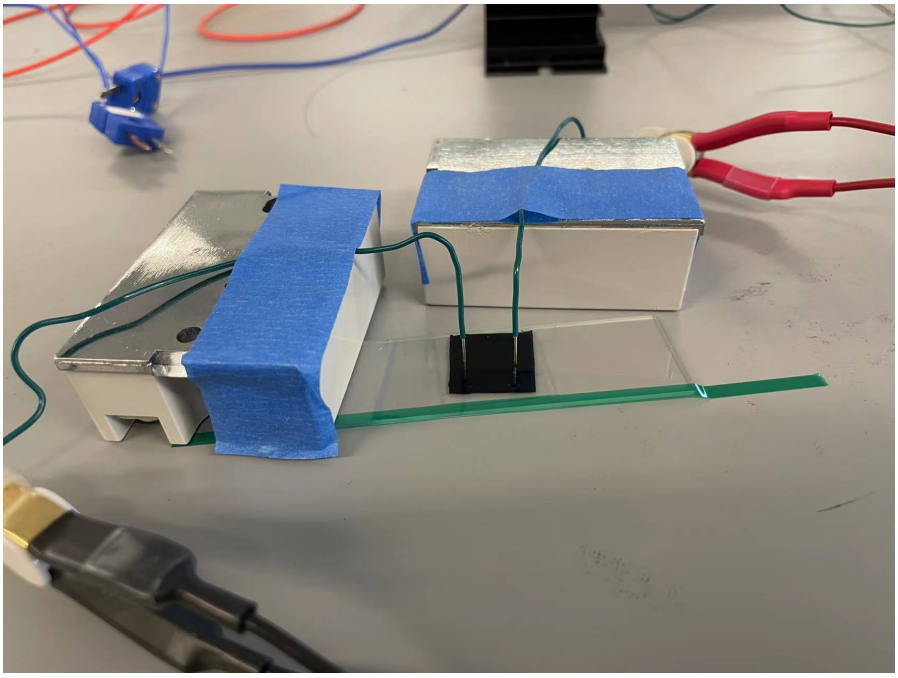

Figure 7: Self-designed four-probe method apparatus for electrical conductivity measurement

sample while measuring, which allows for a more accurate average value when taking multiple measurements on one sample.

What's more, in order to calculate the resistivity then the electrical conductivity, we also need to know the space between each probe and the thickness of the sample. For bulk samples, we performed both space and thickness measurement by using a precise caliper. But for film samples, due to their really small thickness within micro-scale or nano-scale, instruments with higher accuracy were needed to perform the measurement. Therefore we chose the Keyence

VK-X260 Laser-Scanning Profilometer in CCMR which is an optimal tool for optically profiling a sample's surface with excellent vertical (as low as 5nm) and lateral resolution (Fig.8). It has the ability of measuring pretty thin film samples'

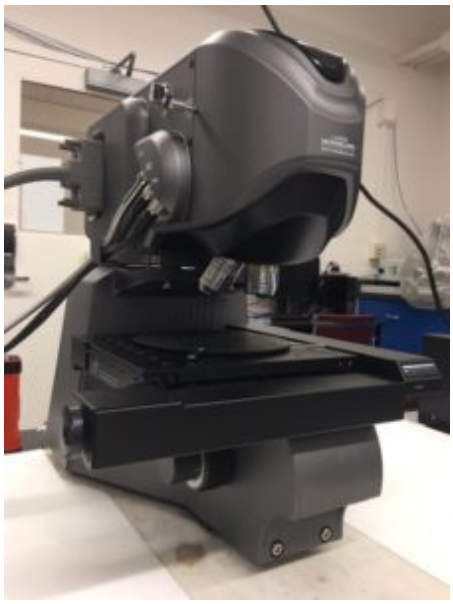

Figure 8: Keyence VK-X260 Laser-Scanning Profilometer

thickness and basically all the thickness data of PEDOT:PSS film in my research is from this instrument.

Move to the Seebeck coefficient part, the measurement apparatus here is much more complicated compared to the four-probe one. After conducting a lot of research, our final design mainly draws on this paper (Bernhard Dörling, 2020) [23]. The first step is about the sample holder design. Two separate copper blocks were manufactured by hand using conventional milling with the same size of 45 mm × 20 mm × 16 mm (Fig.9). The sample is supported face down on two blocks forming a bridge shape. Left copper block works as the heat source which includes a horizontally oriented channel specifically designed to securely accommodate the cartridge heater. Additionally, it features a threaded

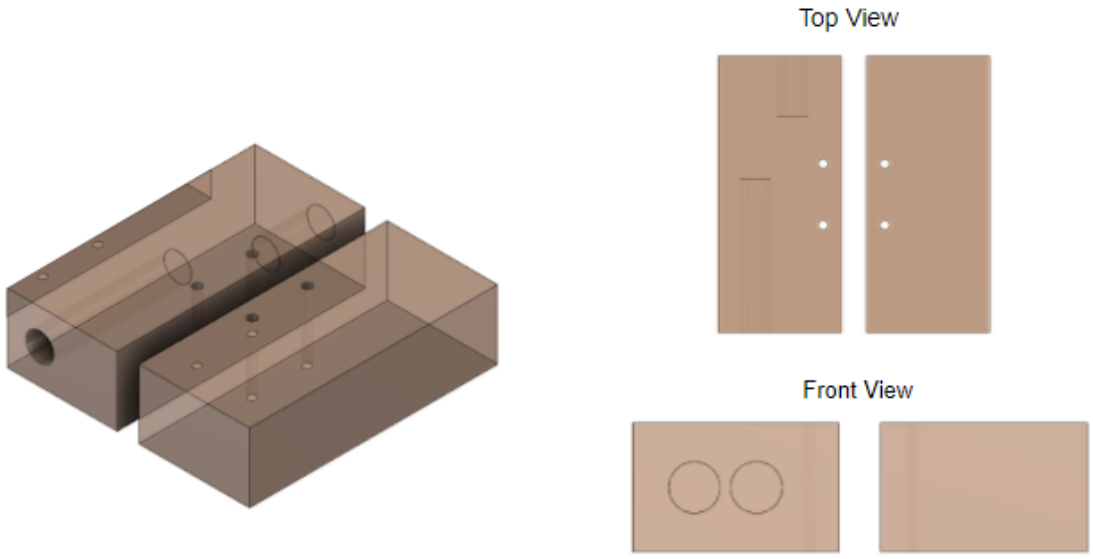

Figure 9: Three views of the sample holder

hole of smaller length at the back intended for the K-Type screw thermocouple utilized for PID sensing. Right copper block works as the heat sink and both of these two blocks contain two vertical channels each to mount copper-constantan (T-type) thermocouples with upward-facing measurement junctions to measure the sample.

Moving on to the next step, in order to measure the Seebeck coefficient, we need to have a constant temperature gradient between the heat source and heat sink which means the cartridge heater needs to be controllable. Therefore a system is designed to meet that purpose (Fig.10). The system contains a 40W, 24V cartridge heater, a Inkbird ITC-106VL proportional-integral-derivative(PID) Temperature Controller, a DMWD 25A DC-DC Solid State Relay(SSR), a screw K-type thermocouple and a Extech 382213 DC Regulated Power Supply (Fig.11). The SSR driven by a PID controller regulates the cartridge heater. The PID controller measures the current temperature of the hot

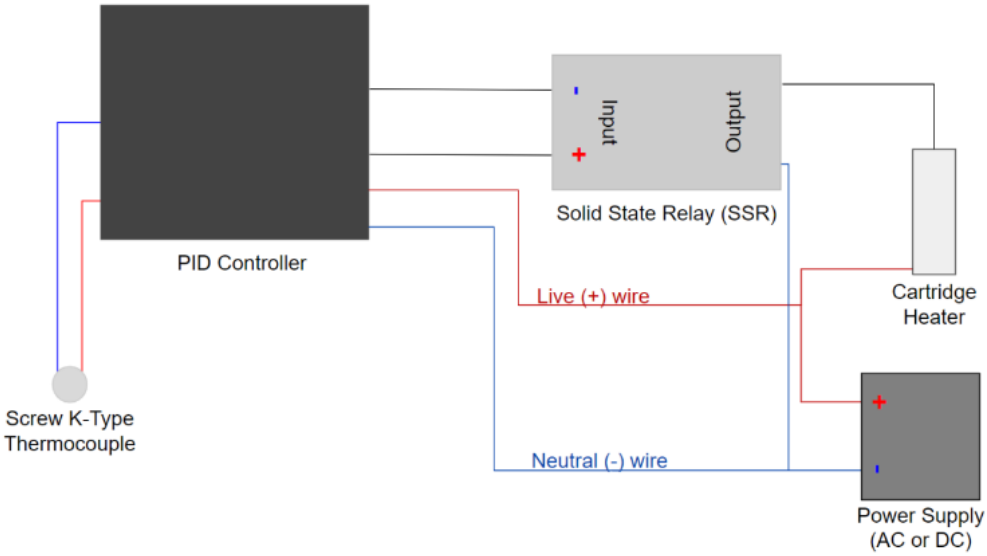

Figure 10: Control system wiring map for cartridge heater

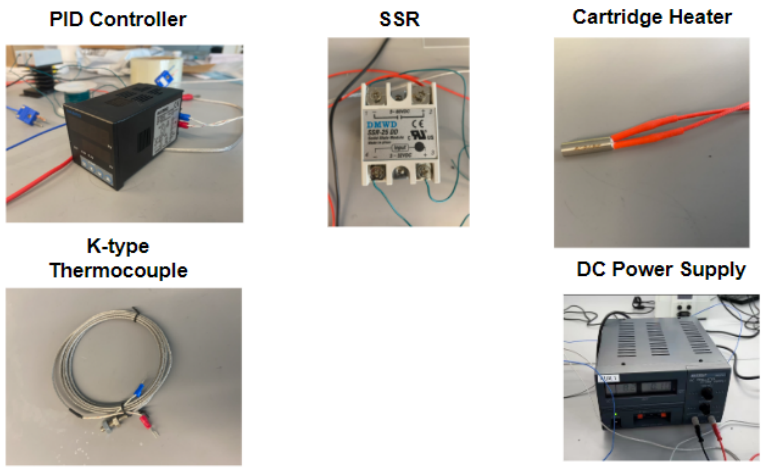

Figure 11: Control system's components

side using the K-type thermocouple and adjusts the power supplied to the heater via electronic on/off switching facilitated by the relay. Both the SSR and the PID controller are connected to a DC power supply operating at approximately 18 V, which provides the necessary voltage for the heater.

After combining the cartridge heater system, sample holder and thermocouples, the main part of the Seebeck coefficient measurement apparatus is shown in (Fig.12). The cardboard box works as the support for the sample holder and allows T-type thermocouples to pass from bottom to top. However, these few

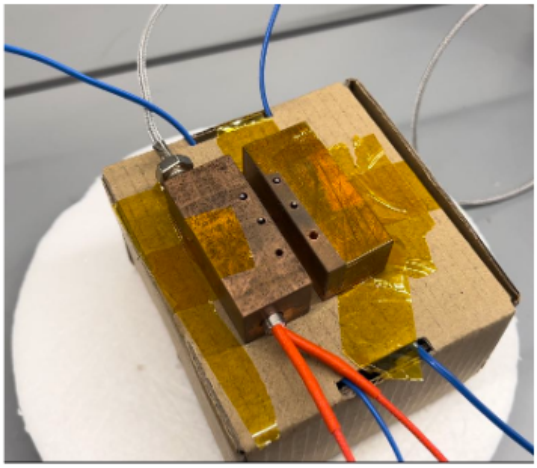

Figure 12: Control system's components

things alone are not enough to perform measurement. In order to record the data including temperature at different sides and the voltage between thermocouples, a digital thermometer and a voltmeter are necessary. Here, we use the KEITHLEY 2450 Sourcemeter as the voltmeter. Therefore, the overall layout of the Seebeck coefficient measurement apparatus looks like this (Fig.13).

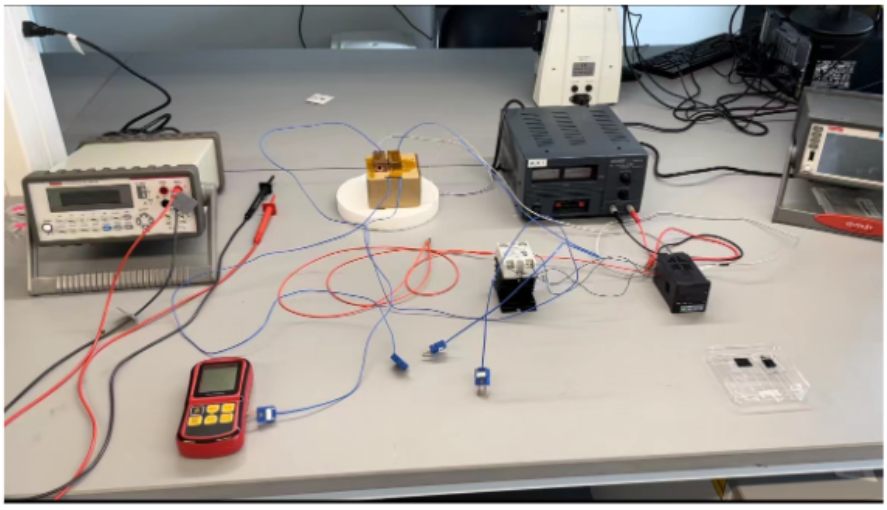

Figure 13: Overall Layout of the actual apparatus for Seebeck coefficient measurement

3.4 Procedures

The procedures section outlines the systematic and detailed steps undertaken to conduct the research which is crucial for establishing the credibility and replicability of the research, ensuring that others can follow the same steps to validate or build upon the findings presented in this thesis. This section consists of three main processes, the design measurement apparatus verification process, film fabrication process and thermoelectric properties optimization process.

3.4.1 Designed measurement apparatus verification

The verification process for the designed measurement apparatus involves a comprehensive evaluation to ensure their accuracy, reliability, and consistency. The whole process includes the measurement of two samples, first one is the

bismuth telluride (Bi_2Te_3) bulk sample from Ren Group at University of Houston and the second one is a pristine PEDOT:PSS film sample from He Group at University of California Los Angeles (UCLA). Since there were a total of two apparatus to verify, we measured both electrical conductivity and Seebeck coefficient of these two samples and compared the value with their two groups.

(Fig.14) is the measuring process for Bi_2Te_3 bulk sample. Figure (a) shows the four-probe method of electrical conductivity measurement and in figure (b), the sample was placed on the Seebeck coefficient measurement apparatus and fixed by the Kapton tape on a glass substrate. After several measurements, the

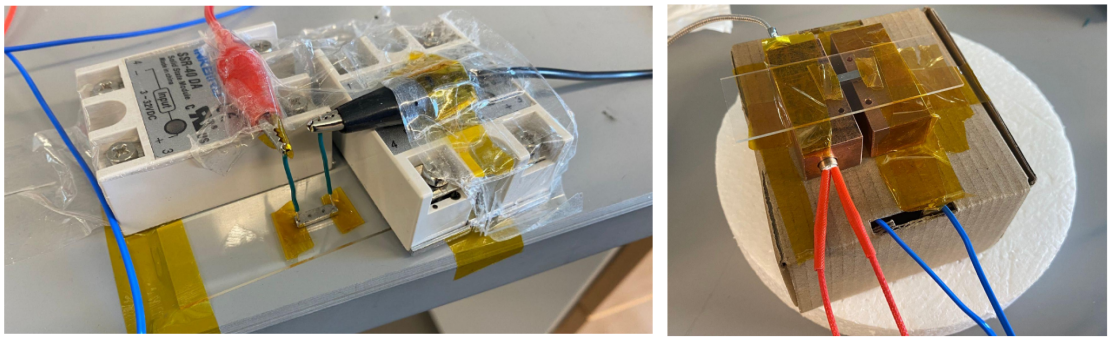

(a) Electrical conductivity measurement (b) Seebeck coefficient measurement

Figure 14: Measuring process for Bi_2Te_3 bulk sample

final averaged data are shown in the following tables.

Properties	**values**
Sample Thickness t (m)	1.7e-03
Sample Resistance R (Ω)	2.44e-03
Probe Spacing s (mm)	2.35
Resistivity ρ (Ωm)	1.83e-05
Electrical Conductivity σ (S/cm)	548

Table 1: Measured electrical conductivity of the Bi_2Te_3 bulk sample

Temperature (C)	**Seebeck Coefficient (μV/K)**
26.7	193.8
29.4	194.9
31.2	195.6
32.9	196.3
34.9	197.1

Table 2: Measured Seebeck coefficient of the Bi_2Te_3 bulk sample around room temperature

In order to ensure the credibility of the verification process, we didn't know the actual value of the sample before the measurement results were obtained, but sent them to the two groups for comparison after the end. For the Bi_2Te_3 bulk sample, Ren group's values are 581 S/cm of electrical conductivity and 199 μV/K of Seebeck coefficient at room temperature. According to the small

variance, the apparatus verification succeeded when dealing with the bulk sample.

The measurement for the pristine PEDOT:PSS film sample from He Group has also been carried out using the same apparatus. (Fig.15) shows the measuring process. Also multiple measurements has been performed and the final

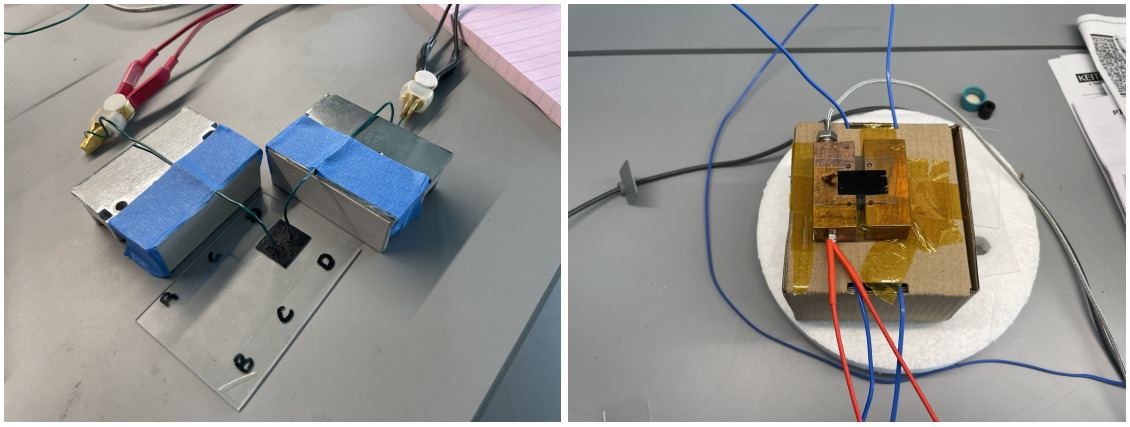

(a) Electrical conductivity measurement (b) Seebeck coefficient measurement

Figure 15: Measuring process for pristine PEDOT:PSS film sample

averaged data are shown in Table 3 and Table 4.

For the pristine PEDOT:PSS sample, He Group has provided us with two value ranges which are 0.1-10 S/cm of electrical conductivity and 12-18 μV/K of Seebeck coefficient at room temperature. Both of our values stay within the range hence the apparatus verification also succeeded when dealing with the film sample.

Properties	values
Sample Thickness t (m)	5e-05
Sample Resistance R (Ω)	1.48e06
Resistivity ρ (Ωm)	7.41e-03
Electrical Conductivity σ (S/cm)	1.35

Table 3: Measured electrical conductivity of the pristine PEDOT:PSS film sample

Temperature (C)	Seebeck Coefficient (μV/K)
29.4	12.9
31.5	13.0
33.4	13.0
34.9	13.1
35.9	13.1

Table 4: Measured Seebeck coefficient of the pristine PEDOT:PSS film sample around room temperature

3.4.2 Film sample fabrication

PEDOT:PSS is usually kept in aqueous dispersion form and there are plenty of techniques of fabricating its films. In my research, I mainly adopted the two most commonly used, spin coating technique and drop casting technique. Spin coating technique involves the deposition of a thin, uniform layer of material

onto a substrate through centrifugal force [24]. This technique is commonly employed in various fields, including microelectronics, optics, and nanotechnology. The process begins by applying a small quantity of liquid precursor or solution onto the center of the spinning substrate in a spin coater. As the substrate rapidly rotates, the centrifugal force spreads the liquid over its surface, resulting in a thin film with controlled thickness [24]. The spinning speed and duration which can be set on the spin coater are crucial parameters that determine the film's thickness and quality. Spin coating offers several advantages, such as simplicity, versatility, and the ability to achieve thin films with excellent uniformity and smoothness. (Fig.16) is a picture of the spin coater we use in our lab. Compared with spin coating, drop casting is a relatively simpler and

Figure 16: The Laurell WS-650-23 B spin coater

low-cost technique that does not require the assistance of equipment. The process involves placing a solution or dispersion containing the desired material onto a substrate, typically through pipetting or dropper dispensing [25]. As the

droplets come into contact with the substrate, the solvent begins to evaporate, leaving behind a thin film of the material. The film's thickness and uniformity can be influenced by factors such as droplet size, solution concentration, and substrate properties [25]. Drop casting is a straightforward and cost-effective method for producing thin films, making it suitable for various research and manufacturing applications. However, it may result in less uniform films compared to other techniques, and control over film thickness can be more challenging. Nonetheless, drop casting remains a valuable tool for thin film fabrication and offers flexibility in terms of materials and substrates that can be utilized.

Either spin coating or drop casting, in order to make a high quality PEDOT:PSS film, the first step of the fabrication process is always substrate cleaning. It takes about 2 hours to clean up a batch of substrates which can be divided into 5 small steps: 1. 30 mins IPA (Isopropyl Alcohol) treatment under ultrasonication; 2. 30 mins Acetone treatment under ultrasonication; 3. 30 mins DI water treatment under ultrasonication; 4. Dry the chosen substrates using filtered compressed gas; 5. Place the chosen substrates into the UV oZone cleaner (Fig.17) and leave for 15-30 mins (no less than 15 mins).

Figure 17: Ossila UV ozone cleaner in the lab

After the substrate cleaning process, we can start making the film. Pure PEDOT:PSS (Clevios PH1000) aqueous dispersion was purchased from Ossila (Fig.18). During the spin coating process, 70μL of PEDOT:PSS was dropped on

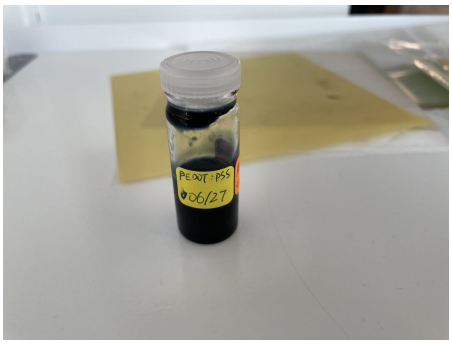

Figure 18: Pure PEDOT:PSS (Clevios PH1000) aqueous dispersion

a 1.5cm × 1.5cm glass substrate by the mechanical pipette and placed on the Laurell spin coater. The spinning was set at 1600 rpm and the duration was 30 seconds. After spin coating, the sample was annealed on a hot plate at 80 °C for 30 mins and became full dried. The thickness of the spin coated pure PEDOT:PSS film sample was around 100 nm.

The drop casting technique was carried out by dropping 300μL of PEDOT:PSS aqueous dispersion directly on the glass substrate. Since the substrate surface was treated by UV ozone cleaner before, it became more hydrophilic and had less contact angle which was easier for the liquid to spread. The sample was then annealed on a hot plate at 80 °C for 30 mins and became full dried. The thickness of the drop casted pure PEDOT:PSS film sample was around 10 μm. The actual appearance of the fabricated film sample is shown in the figure below (Fig.19).

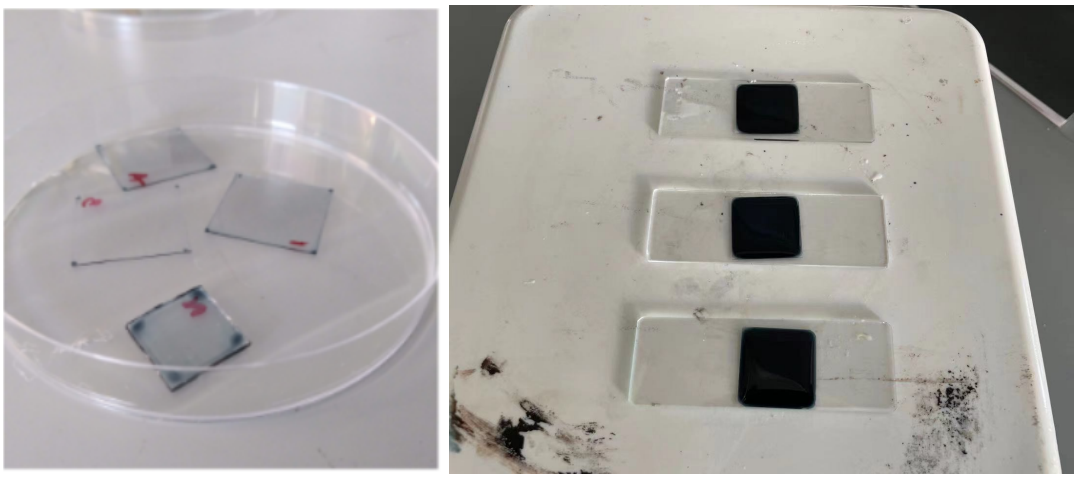

(a) Spin coated films in the petri dish (b) Drop casted films on the hot plate

Figure 19: Fabricated pure PEDOT:PSS film samples

3.4.3 Thermoelectric properties optimization

Thermoelectric properties optimization process is the most important part of the procedures section. Because pure PEDOT:PSS film itself has a really low power factor compared to inorganic thermoelectric materials, it cannot be applied in practice without optimization. Since the project is for building the OTEG, spin coated nanofilms are too thin to form OTEG couples, therefore optimizing the drop casted PEDOT:PSS films becomes the primary target. As I mentioned in the literature review chapter, there are many ways to improve PEDOT:PSS's thermoelectric properties, but the most convenient, quick and efficient approaches are doping and post-treatment (Fig.20). The doping approach is performed by adding additional compounds into PEDOT:PSS aqueous solution, such as polar organic solvents, acid or base, anionic surfactants, and ionic liquids. So firstly make a mixture of solution and follow by the spin coating or drop casting method to prepare the film sample. Doping these compounds would increase the charge carrier concentration and induce strong phase seg-

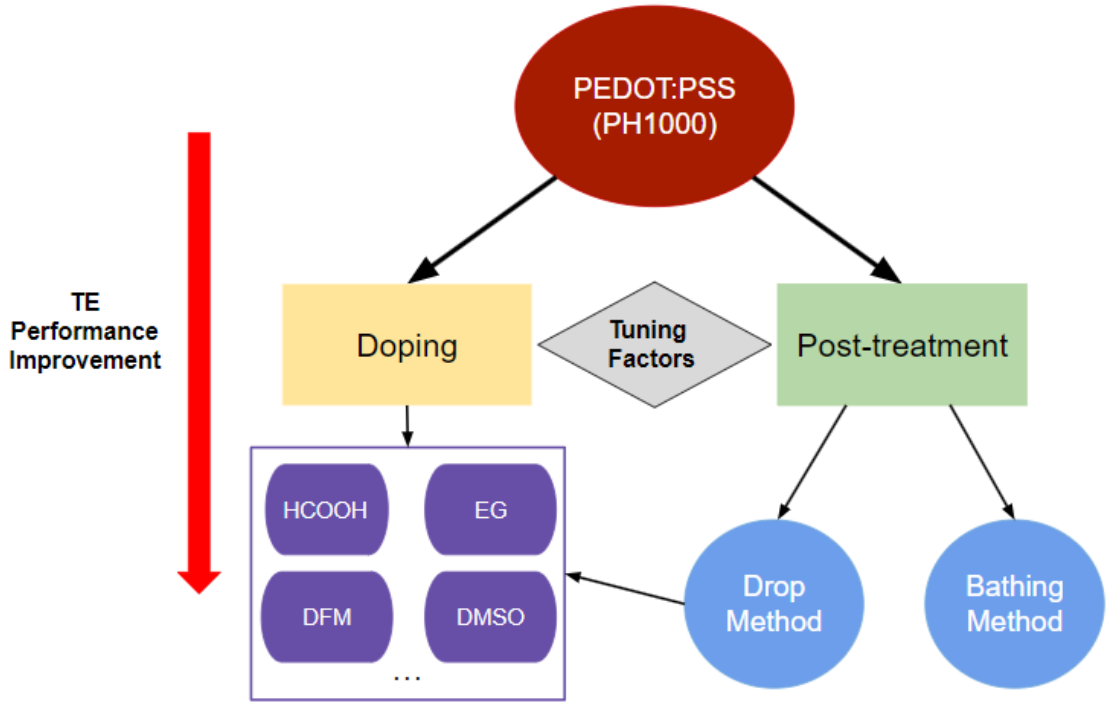

Figure 20: Concept map for optimizing PEDOT:PSS thermoelectric properties

regation therefore increase the electrical conductivity and Seebeck coefficient [10]. The post-treatment approach is carried out by immersing the annealed PEDOT:PSS film into several polar solvents (Bathing Method) or dropping a small amount of liquid directly on the PEDOT:PSS film (Drop Method) at a certain temperature [10,26]. And the last step is to rinse with DI water and bake it, which can also be seen as another heat annealing process until the sample is fully dried. A variety of materials have been reported for the post-treatment process such as DMSO, EG, Formanide and so on. The post-treatment approach can improve the electrical conductivity by removing the insulating PSS. In PEDOT:PSS films, the PEDOT-rich core is generally surrounded by a PSS-rich shell. Following the post-treatments, the inefficient PSS is removed, which leads to strong phase segregation, and the PEDOT-rich grains are interconnected. And

then higher electrical conductivity and Seebeck coefficient.

At the beginning phase of the research, I tried the two approaches separately and found that they have indeed improved the performance of PEDOT:PSS, especially the electrical conductivity, which has been significantly improved. For the doping approach, 10 vol% of N,N-Dimethylformamide (DFM) and 10 vol% of formic acid (HCOOH) was used separately as the dopant. The procedure is shown in (Fig.21). As for the post-treatment approach, I have tried the

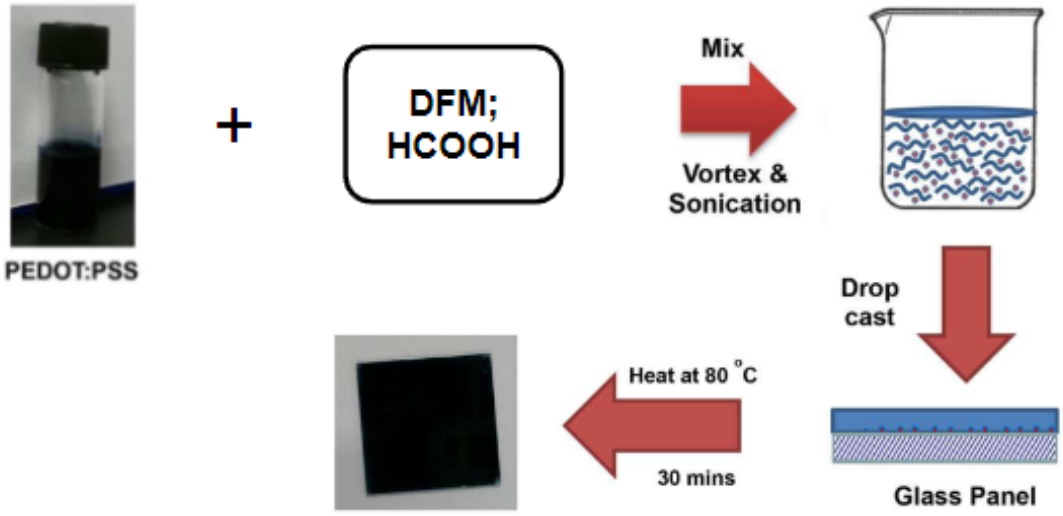

Figure 21: Doping approach on PEDOT:PSS using DMF and Formic acid

drop method also with two different chemicals, which were dimethyl sulfoxide (DMSO) and zinc chloride ($ZnCl_2$). The procedure is shown in (Fig.22).

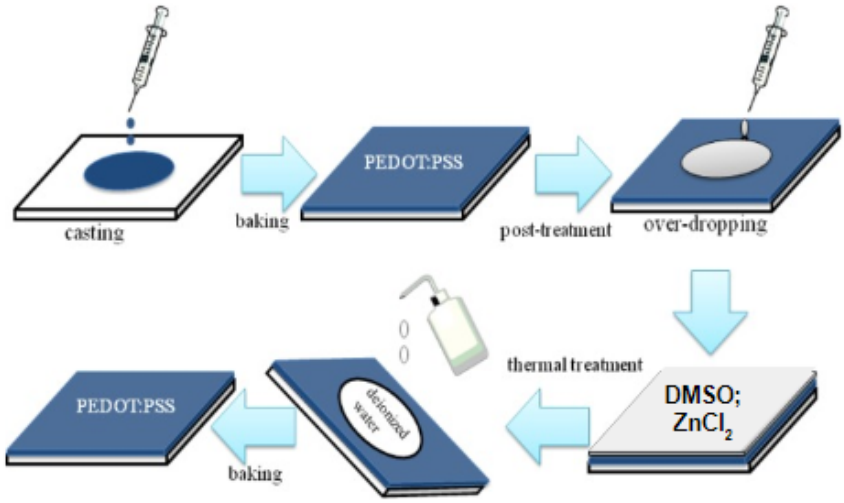

Figure 22: Drop method of post-treatment approach on PEDOT:PSS using DMSO and $ZnCl_2$

Although the result is not bad, the improvement of the power factor has not achieved what I expected. Therefore another experiment was set up, which is more systematic and with controlled variables. This time, in order to reach a higher value of power factor, a combination approach combined with doping and post-treatment applied to the PEDOT:PSS film samples. The candidate chemicals were DMSO and ethylene glycol (EG), the two most commonly used organic solvents. What's more, during the experiment, we found that by immersing the PEDOT:PSS film into the EG solution, the film would automatically peeled off from the substrate and became free-standing. Free-standing PEDOT:PSS films offer a lot of advantages such as flexibility which means they're transferable and foldable. So this time, I chose the bathing method of post-treatment within the combination approach. So the whole process consisted of two steps, the first step is doping PEDOT:PSS aqueous dispersion with DMSO and EG separately at different doping levels, 5 vol%, 10 vol%, 15 vol% respectively (Fig. 23). The second step turned to the post-treatment approach. After

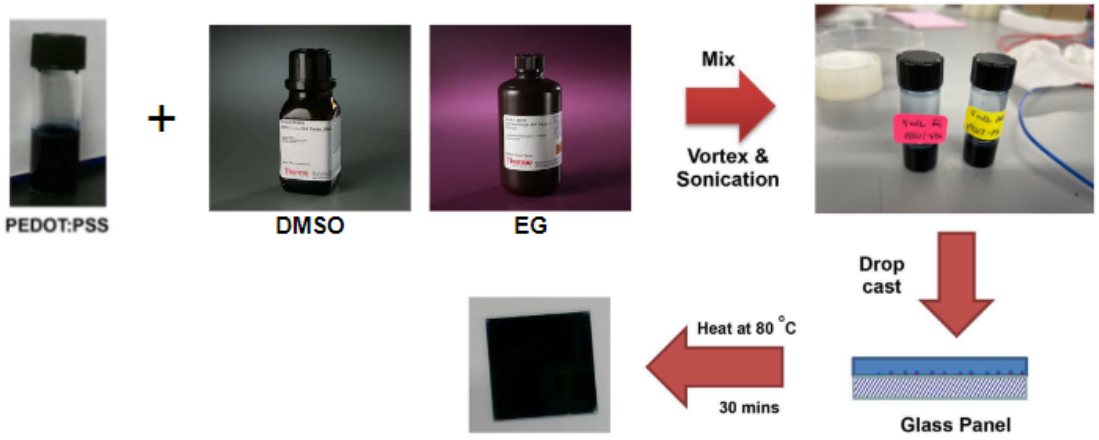

Figure 23: First step of combination method (Doping approach)

the heat annealing process for the doped film samples, the bath method of post-treatment was applied by immediately immersing the samples in an EG bath (kept at 60°C for EG-doped PEDOT:PSS and at room temperature for DMSO-doped PEDOT:PSS) for a certain length of time. The EG bathing times at this step were 60 mins, 120 mins, 180 mins, 240 mins, and 300 mins respectively (Fig.24). During the EG bathing, PEDOT:PSS films would become totally free-

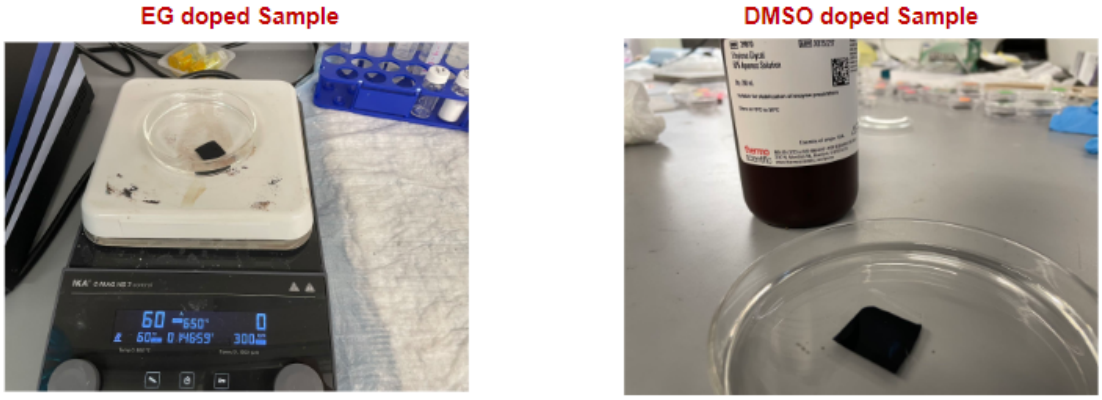

Figure 24: Second step of combination method (Post-treatment approach)

standing. Then they would be rinsed by the DI water and transferred to larger glass substrates. After the films were fully dried inside the fume hood, necessary measurement and data analysis would be taken.

3.5 Data Analysis

In order to compare PEDOT:PSS samples' thermoelectric performance, the most important thing is to get a credible power factor value which is calculated from electrical conductivity and Seebeck coefficient, therefore data from the measurement process needs to be analyzed. This section consists of two parts, electrical conductivity analysis and Seebeck coefficient analysis.

3.5.1 Electrical conductivity analysis

The data analysis for electrical conductivity of PEDOT:PSS film samples was quite simple. The thickness data was from the Keyence VK-X260 Laser-Scanning Profilometer and the film resistance was measured through the four-probe apparatus. During the resistance measurement, the sourced current was kept at 1 mA from the two outer probes. What's more, each sample was measured at least five times with probes at different locations on the surface and then the average value and error of the electrical conductivity are obtained through simple calculations (Eq.6).

3.5.2 Seebeck coefficient analysis

The Seebeck coefficient is determined by measuring the temperatures and voltages from both copper (Cu) and constantan (Co) ends of each T-type thermocouple. At each specified temperature, the corresponding voltages V_{Cu} and V_{Co} are recorded and reported alongside the hot and cold block temperatures (T_{hot}, T_{cold}). The Seebeck coefficient, S(T), is calculated using (Eq.8)[23].

$$S(T) = \frac{S_{Cu}(T) - S_{Co}(T)}{1 - \frac{\partial V_{Cu}T}{\partial V_{Co}T}} + S_{Co}(T) \tag{8}$$

Where $\frac{\partial V_{Cu}T}{\partial V_{Co}T}$ is obtained by performing a simple linear regression analysis on the copper and constantan Seebeck voltages plotted against each other for each measured temperature. The effect of the copper and constantan thermocouple ends on the measured Seebeck voltage are accounted for with the above first-order approximation using their respective Seebeck coefficients, $S_{Cu}(T)$ and $S_{Co}(T)$, which can be obtained from the established empirical temperature-dependent correlations in (Eq.9), (Eq.10), (Eq.11) [27, 28].

$$S_{Cu}(T) = 0.041T[exp(-\frac{T}{93}) + 0.123 - \frac{0.442}{1 + (\frac{T}{142.4})^3}] + 0.804 \tag{9}$$

$$\begin{aligned} S_{Cu/Co}(T) = 4.37184 + 0.1676T - (1.84371 \times 10^{-4})T^2 \\ +(1.2244 \times 10^{-7})T^3 - (4.47618 \times 10^{-11})T^4 \end{aligned} \tag{10}$$

$$S_{Co}(T) = S_{Cu}(T) - S_{Cu/Co}(T) \tag{11}$$

$S_{Cu/Co}(T)$ is the Seebeck coefficient of the T-type (copper-constantan) thermocouple. For all the correlations mentioned above, the temperature T denotes the

average temperature obtained by measuring between the hot and cold copper blocks. It is calculated as $T = \frac{T_{hot}+T_{cold}}{2}$. Therefore, this average temperature represents the specific temperature at which is determined for the sample in each set temperature. For the Seebeck coefficient measurement process, each sample was measured more than 3 times and and then the average value and error were obtained.

CHAPTER 4

RESULTS

This chapter reports the result of the study. The findings from the data collection process are presented here including initial attempts and subsequent systematic experiments. The results in this chapter will provide insights into the effectiveness of the proposed optimization strategies and the overall thermoelectric efficiency achieved.

4.1 Optimization process initial attempts results

The electrical conductivity measurement through four-probe apparatus and Seebeck coefficient measurement through designed apparatus has been performed on all four PEDOT:PSS film samples, two were doped and the other two were post-treated. So the results including the calculated power factor of the first two samples which were doped with DFM and HCOOH separately is shown (Table.5).

Samples	$\sigma(S\,cm^{-1})$	$S(\mu VK^{-1})$	$PF(\mu Wm^{-1}K^{-2})$
Pristine PEDOT:PSS	~0.455	~17.3	~0.0136
PEDOT:PSS doped with 10 vol% DFM	322	32.3	33.6
PEDOT:PSS doped with 10 vol% HCOOH	393	29.0	33.1

Table 5: PEDOT:PSS (PH1000) doping approach result

And the results of the rest two samples which were post-treated with DMSO and $ZnCl_2$ separately using drop method is shown (Table.6). It is not difficult to see

Samples	$\sigma(S\,cm^{-1})$	$S(\mu VK^{-1})$	$PF(\mu Wm^{-1}K^{-2})$
Pristine PEDOT:PSS	~0.455	~17.3	~0.0136
PEDOT:PSS post-treated with DMSO	853	18.3	28.6
PEDOT:PSS post-treated with $ZnCl_2$	485	24.5	29.1

Table 6: PEDOT:PSS(PH1000) post-treatment approach result

from these tables that the effect of improving PF by using one certain approach, either doping or post-treatment, is similar, and the difference is due to different chemical substances. Compared with the pristine PEDOT:PSS, both two approaches greatly improved the electrical conductivity, which was three orders of magnitude higher. The Seebeck coefficient had also been slightly improved. The PEDOT:PSS sample that was post-treated with DMSO got the highest value of electrical conductivity among all four samples, the one doped with 10 vol% HCOOH got the highest Seebeck coefficient and also the highest power factor among all four samples.

4.2 Optimization process systematic experiment result

The result of all PEDOT:PSS samples with different trials of treatment within the experiment will be presented here. Due to the EG bathing method of post-treatment that the film samples were totally immersed in the solution, the thick-

ness of them has been reduced a lot (removing of excess PSS). The degree of thickness reduction is shown below through (Table.7) to (Table.9).

Thickness (μm)	**PEDOT:PSS doped with 5 vol% DMSO**	**PEDOT:PSS doped with 5 vol% EG**
0 mins of EG bath	8.31	13
60 mins of EG bath	5.61	7.94
120 mins of EG bath	4.32	4.91
180 mins of EG bath	4.19	4.5
240 mins of EG bath	4.04	4.29
300 mins of EG bath	3.48	3.87

Table 7: PEDOT:PSS film samples' (with 5 vol% doping level) thickness reduction after post-treatment

Thickness (μm)	**PEDOT:PSS doped with 10 vol% DMSO**	**PEDOT:PSS doped with 10 vol% EG**
0 mins of EG bath	7.65	12.4
60 mins of EG bath	6.51	8.56
120 mins of EG bath	5.33	5.93
180 mins of EG bath	4.12	3.87
240 mins of EG bath	3.98	3.39
300 mins of EG bath	3.88	3.29

Table 8: PEDOT:PSS film samples' (with 10 vol% doping level) thickness reduction after post-treatment

Thickness (μm)	PEDOT:PSS doped with 15 vol% DMSO	PEDOT:PSS doped with 15 vol% EG
0 mins of EG bath	8.73	10.6
60 mins of EG bath	6.21	8.14
120 mins of EG bath	4.89	5.86
180 mins of EG bath	4.35	4.66
240 mins of EG bath	2.62	3.49
300 mins of EG bath	2.48	3.30

Table 9: PEDOT:PSS film samples' (with 15 vol% doping level) thickness reduction after post-treatment

The tables provide valuable insights into the thickness variations of the DMSO and EG doped samples at different doping levels, as influenced by the duration of EG bathing. A consistent observation is that an increase in EG bathing time corresponds to a reduction in sample thickness. This trend continues until the thickness stabilizes at approximately 3 micrometers.

The thickness data of these samples with the four-probe apparatus lead to the electrical conductivity result, which is shown in the plots below (Fig.25).

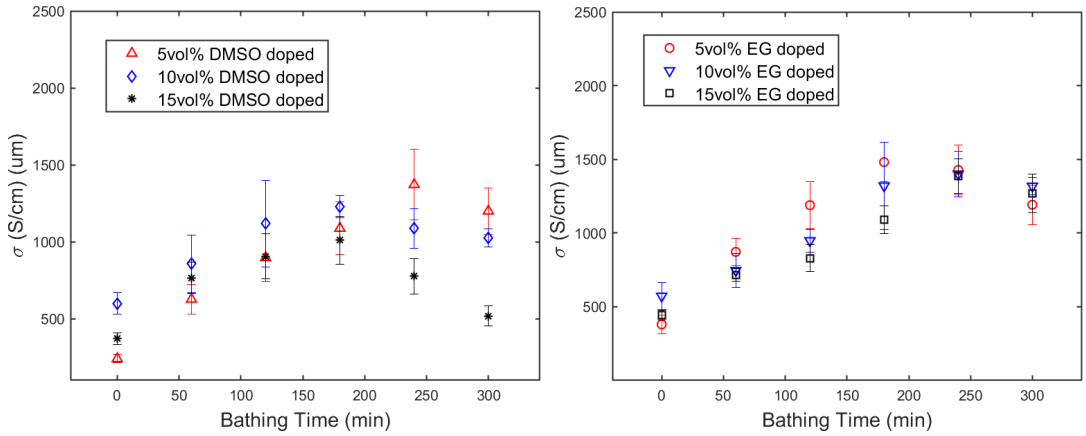

(a) All DMSO doped samples (b) All EG doped samples

Figure 25: Electrical conductivity result plot of PEDOT:PSS film samples

The electrical conductivity trend observed in both the DMSO and EG doped samples displays a remarkable similarity. The initial conductivity values, prior to post-treatment, are already quite substantial, hovering around 500 S/cm. Subsequently, as the EG bathing time increases, the conductivity experiences a steady rise until it reaches a specific threshold around 180 minutes. Beyond this point, however, the electrical conductivity starts to decline with further increases in the EG bathing time. Notably, the DMSO doped sample demonstrates the highest conductivity value, peaking at 1373 S/cm when subjected to a 5 vol% doping level and an EG bathing duration of 240 minutes. On the other hand, the EG doped sample achieves its highest conductivity level at 1481 S/cm, also with a 5 vol% doping level, but at a slightly shorter EG bathing time of 180 minutes. These findings highlight the influence of both doping level and EG bathing time on the electrical conductivity of the samples, underscoring the significance of optimizing these parameters for desired conductivity outcomes.

Next is the Seebeck coefficient results of all the samples, the plot is shown in (Fig.26). The plot depicts the Seebeck coefficient with respect to EG bathing

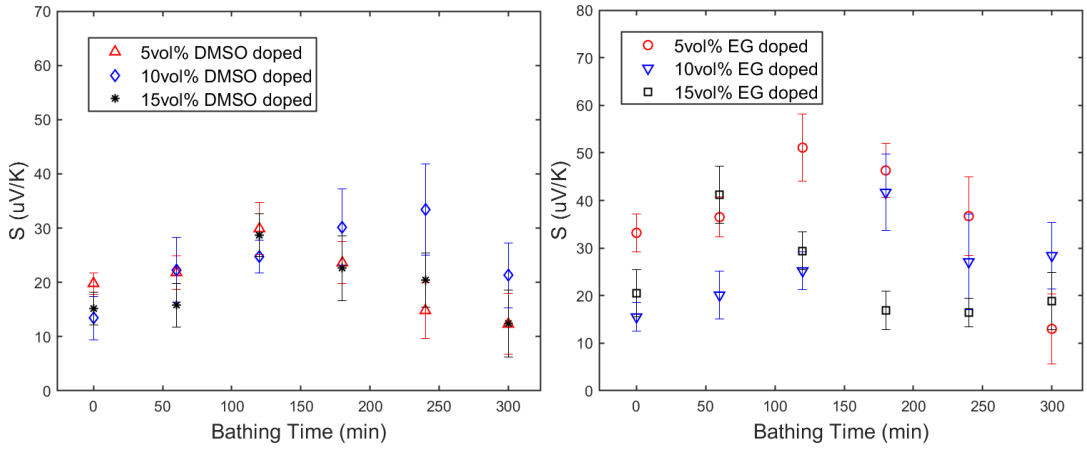

(a) All DMSO doped samples (b) All EG doped samples

Figure 26: Seebeck coefficient result plot of PEDOT:PSS film samples

time, also showcasing a trend of initially increasing and then gradually decreasing. The Seebeck coefficient, a measure of the thermoelectric properties of a material, starts with a promising rise as the EG bathing time increases. This upward trend suggests an enhancement in the material's ability to convert temperature differences into electrical energy. As the EG bathing time continues to advance, the Seebeck coefficient reaches its peak, indicating an optimal performance level. However, beyond this peak, the trend shifts, and the Seebeck coefficient begins to decline. This decrease signifies a decline in the material's thermoelectric efficiency, potentially due to the onset of certain limitations or degradation mechanisms associated with prolonged post-treatment using organic solvents. The highest Seebeck coefficient value for DMSO doped samples is at 33.4 μV/K with 10 vol% doping level and 240 mins of EG bathing. As for EG doped samples, their Seebeck coefficient values are generally higher compared with DMSO doped, peaking at 51.1 μV/K when subjected to a 5 vol% doping level and 120 mins of EG bathing.

Combining the electrical conductivity result with the Seebeck coefficient re-

sult, the final power factor result of PODOT:PSS film samples appears. (fig.27). The power factor plot exhibits a similar trend to the Seebeck coefficient plot, and

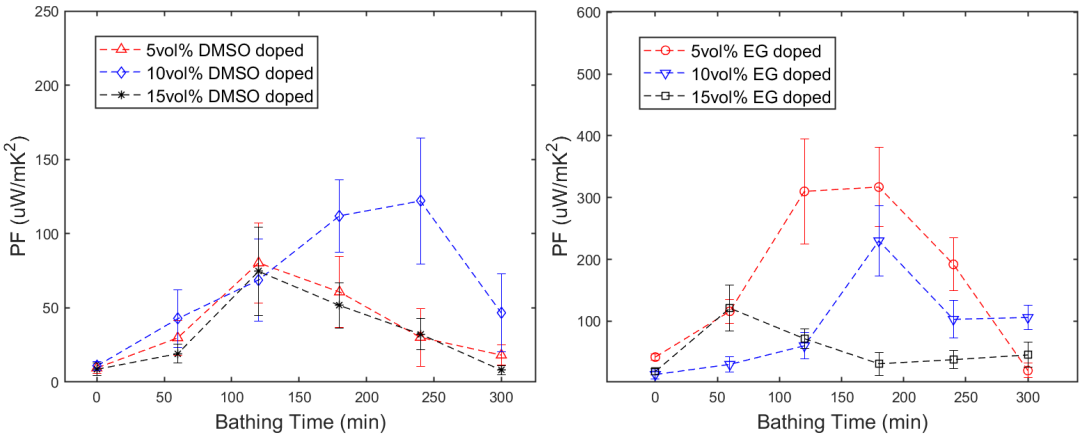

(a) All DMSO doped samples (b) All EG doped samples

Figure 27: Power factor result plot of PEDOT:PSS film samples

this correlation can be attributed to the mathematical relationship between the two. In the calculation of power factor, the Seebeck coefficient is squared. Consequently, any changes or improvements in the Seebeck coefficient have a more pronounced effect on the power factor compared to changes in electrical conductivity alone. This indicates that enhancing the Seebeck coefficient is a more efficient strategy for improving the overall power factor. As the Seebeck coefficient initially increases with EG bathing time, it leads to a significant rise in the power factor, reflecting the enhanced thermoelectric performance. However, as the EG bathing time continues to progress, the Seebeck coefficient reaches its peak, and subsequent changes start to have diminishing returns, resulting in a gradual decline in the power factor. For DMSO doped sample, highest power factor is at 122 μW/mK^2 with 10 vol% doping level and 240 mins of EG bathing (Same as the highest Seebeck coefficient data point). And the overall highest power factor, 317 μW/mK^2, is obtained by the EG doped sample with 5 vol%

doping level and 180 mins of EG bathing since EG seems to better at optimizing the Seebeck coefficient. Therefore, by focusing on enhancing the Seebeck coefficient while keeping electrical conductivity stays the same, researchers can achieve more efficient improvements in the power factor and, subsequently, in the overall performance of thermoelectric systems.

CHAPTER 5

DISCUSSION

The last chapter of the thesis will discusses the results from last chapter and draws conclusions about the study's findings. The discussion also evaluates the effectiveness of the optimization strategies employed and provides insights into further improvements and future directions for research. There're total of three sections in this chapter, which are conclusion, limitation and future expectations.

5.1 Conclucion

The combination method of doping approach and post-treatment approach was employed to optimize the power factor of the PEDOT:PSS film. The best results among all samples demonstrated a significant improvement in the power factor from about 0.0136 $\mu W/mK^2$ (pristine PEDOT:PSS film) to 317 $\mu W/mK^2$ at room temperature. This achievement was primarily attributed to the high electrical conductivity (1481 Scm-1) and Seebeck coefficient (46.3 µVK-1) obtained after doping the film with 5 vol% of EG and subjecting it to a 3-hour EG bathing post-treatment.

The results obtained in this study provide evidence that the combination method of doping approach and post-treatment approach is more effective in optimizing the thermoelectric properties of PEDOT:PSS compared to using either approach individually. The synergistic effect of combining these two methods leads to a significant enhancement in the power factor of the PEDOT:PSS

film. While the doping approach alone improves the electrical conductivity of the film, resulting in enhanced charge carrier transport, the post-treatment approach further refines the material's structure and enhances its thermoelectric performance. The post-treatment process, in this case, involved bathing the film in EG for a specific duration. This treatment modifies the film's morphology, reduces impurities, and enhances the intermolecular interactions within the PEDOT:PSS matrix, resulting in improved thermoelectric properties. This finding underscores the significance of a comprehensive and integrated approach when optimizing the thermoelectric properties of materials. By combining multiple methods, researchers can exploit the unique benefits of each approach and achieve superior performance compared to relying on a single method. The effectiveness of the combination method demonstrated in this study provides valuable insights for future research in the field of thermoelectric materials and highlights the importance of exploring synergistic approaches to maximize performance.

Furthermore, the results of this study indicate that the EG-doped samples exhibit better performance in terms of improving the Seebeck coefficient compared to the DMSO-doped samples, although both dopants show similar improvements in electrical conductivity. Additionally, the optimum doping level of EG was found to be within the range of 5 vol% to 10 vol%. Below this range, the doping concentration is insufficient to produce significant improvements in the thermoelectric properties. Conversely, exceeding this range leads to diminishing returns and may even result in deteriorated performance. The optimum doping level represents a balance between maximizing the benefits of dopant incorporation and avoiding excessive dopant-induced perturbations within the material. These findings emphasize the importance of careful optimization and

control of the doping level when enhancing the thermoelectric properties of PEDOT:PSS. Selecting an appropriate dopant material and optimizing the doping concentration can lead to significant improvements in specific thermoelectric parameters such as the Seebeck coefficient. Such knowledge provides valuable guidance for future research and practical applications, ensuring that the desired thermoelectric properties are effectively achieved through appropriate dopant selection and precise control of the doping level.

5.2 Limitaions

Despite the promising results obtained in this study, it is important to acknowledge the limitations and constraints that were encountered during the research process. These limitations provide valuable insights into areas that could be further improved and expanded upon in future studies.

One of the primary limitations of this study was the poor uniformity of the drop-casted PEDOT:PSS films. The drop-casting method, although widely used for its simplicity, often leads to non-uniform film thickness and surface roughness. This non-uniformity can introduce variations in the thermoelectric properties across the film, affecting the overall performance of the material. However, in this study, spin-coating was not utilized due to the requirement for thicker films in the construction of organic thermoelectric generators. Spin-coating typically results in thin films, which may not meet the desired thickness necessary for efficient energy conversion in thermoelectric devices. Therefore, a compromise had to be made, and drop-casting was chosen as the deposition method.

What's more, the investigation focused solely on the effect of organic sol-

vents on the thermoelectric properties of PEDOT:PSS. Other potential dopants or post-treatment methods were not explored, leaving room for further research in this area. It is possible that alternative dopants or different post-treatment approaches could yield even better thermoelectric performance.

Another limitation pertains to the scalability of the optimized PEDOT:PSS films. The synthesis and characterization in this study were focused on small-scale samples, providing insights into the thermoelectric performance at the laboratory scale. However, the successful translation of thermoelectric materials to practical applications requires the ability to produce large-area films with consistent and reproducible properties.

Last but not least, the stability and durability of the optimized PEDOT:PSS films were not thoroughly investigated in this study. Long-term stability is a crucial consideration for the practical application of thermoelectric materials, as they need to maintain their performance over extended periods of operation.

5.3 Future Expectations

The achievements of this study open up exciting possibilities for future research and development in the field of organic thermoelectric materials. Building upon the findings and limitations of this study, several avenues for future exploration can be identified.

Firstly, addressing the issue of film uniformity in drop-casted PEDOT:PSS films should be a priority. Advanced coating techniques, such vacuum filtration or chemical vapor deposition, should be investigated to achieve more uni-

form and controlled film thickness and surface morphology. By improving the uniformity of the films, researchers can minimize variations in thermoelectric properties and enhance the overall performance and reproducibility of the material.

Secondly, exploring alternative dopants and post-treatment methods can provide further opportunities for enhancing the thermoelectric performance of PEDOT:PSS films. Investigating different dopant materials and concentrations, as well as exploring diverse post-treatment approaches, may yield improved electrical conductivity, Seebeck coefficient, and power factor. Exploring novel dopants and post-treatment methods can expand the design space and contribute to the development of even more efficient and versatile organic thermoelectric materials.

Furthermore, investigating the long-term stability and durability of the optimized PEDOT:PSS films is of great importance. Understanding the degradation mechanisms and developing protective coatings or encapsulation strategies can enhance the material's resistance to environmental factors and extend its operational lifetime. Long-term stability studies should consider the effects of temperature, humidity, and other environmental conditions to ensure the reliability and longevity of the organic thermoelectric devices.

Moreover, the integration of PEDOT:PSS films into practical organic thermoelectric generator devices should be a focus of future research. Building and characterizing prototype devices that utilize the optimized PEDOT:PSS films can provide valuable insights into their performance under real operating conditions. Evaluating factors such as output power, efficiency, and stability in practical device configurations will enable a comprehensive understanding of

the material's potential and guide further optimization efforts.

In conclusion, future research in the field of organic thermoelectric materials should aim to overcome the limitations identified in this study and pursue new avenues for advancement. By addressing issues of film uniformity, scalability, stability, and exploring alternative dopants and post-treatment approaches, researchers can further enhance the thermoelectric performance of PEDOT:PSS films. And the integration of these optimized films into practical devices will pave the way for their widespread application in energy harvesting, wearable electronics, and other emerging technologies, contributing to the development of sustainable and efficient energy solutions.

APPENDIX A

MATLAB CODE

```
%Seebeck coefficient data analysis
%Average temperature input
T = 30+ 273;
%Slope value input
Slp = 0.549;

Scu = 0.041*T*(exp(-T/93)+ 0.123 - (0.442/(1+ (T/172.4)^3)))+0.804;
Scc = 4.37184 + 0.1676*T - 1.84371*10^(-4)*T^2 + 1.2244*10^(-7)*T^3;
- 4.47618*10^(-11)*T^4;
Sco = Scu - Scc;
S = ((Scu - Sco)/(1-Slp))+Sco;
disp(Scu)
disp(Sco)
disp(S)
```

```
%Electrical conductivity plot for all DMSO doped samples
x = [0 60 120 180 240 300];
y1 = [242 628 898 1089 1373 1201];
y2 = [600 858 1119 1230 1088 1026];
y3 = [372 767 906 1011 777 520];
err = [28 96.7 155 171 228 151];
err2 = [69.3 188 283 71 129 59];
err3 = [36.8 101 146 154.1 116 64];
plot(x,y1,'^r','MarkerFaceColor','none','MarkerEdgeColor','r','LineWidth',1)
hold on
plot(x,y2,'diamondb','MarkerFaceColor','none','MarkerEdgeColor','b','LineWidth',1)
hold on
plot(x,y3,'*k','MarkerFaceColor','none','MarkerEdgeColor','k','LineWidth',1)
hold on
errorbar(x,y1,err,'^r','MarkerFaceColor','none','MarkerEdgeColor','r','LineWidth',0.5)
errorbar(x,y2,err2,'diamondb','MarkerFaceColor','none','MarkerEdgeColor','b','LineWidth',0.5)
errorbar(x,y3,err3,'*k','MarkerFaceColor','none','MarkerEdgeColor','k','LineWidth',0.5)
legend('5vol% DMSO doped ','10vol% DMSO doped ','15vol% DMSO doped ','fontsize',12)
xlim([0 380])
ylim([0 2400])
set(gca,'linewidth',1)
ylabel('\sigma (S/cm) (um)','fontsize',14)
xlabel('Bathing Time (min)','fontsize',14)
```

```
%Electrical conductivity plot for all EG doped samples
x = [0 60 120 180 240 300];
y1 = [380 872 1189 1481 1428 1192];
y2 = [572 746 948 1320 1400 1318];
y3 = [442 715 829 1090 1385 1270];
err = [64 90.5 159 134 167 132];
err2 = [92.2 114 76.6 295 156 58.7];
err3 = [33.1 42.6 91.1 93.7 118 132];
plot(x,y1,'or','MarkerFaceColor','none','MarkerEdgeColor','r','LineWidth',1)
hold on
plot(x,y2,'vb','MarkerFaceColor','none','MarkerEdgeColor','b','LineWidth',1)
hold on
plot(x,y3,'sk','MarkerFaceColor','none','MarkerEdgeColor','k','LineWidth',1)
hold on
errorbar(x,y1,err,'or','MarkerFaceColor','none','MarkerEdgeColor','r','LineWidth',0.5)
errorbar(x,y2,err2,'vb','MarkerFaceColor','none','MarkerEdgeColor','b','LineWidth',0.5)
errorbar(x,y3,err3,'sk','MarkerFaceColor','none','MarkerEdgeColor','k','LineWidth',0.5)
legend('5vol% EG doped ','10vol% EG doped ','15vol% EG doped ','fontsize',12)
xlim([0 380])
ylim([0 2500])
set(gca,'linewidth',1)
ylabel('\sigma (S/cm) (um)','fontsize',14)
xlabel('Bathing Time (min)','fontsize',14)
```

```
%Seebeck coefficient plot for all DMSO doped samples
x = [0 60 120 180 240 300];
y1 = [19.8 21.8 29.9 23.6 14.8 12.3];
y2 = [13.4 22.3 24.8 30.2 33.4 21.3];
y3 = [15.2 15.8 28.7 22.6 20.4 12.4];
err = [2 3.1 4.8 3.9 5.2 5.6];
err2 = [4 6 3 7 8.4 6];
err3 = [3 4 4 6 5 6.2];
plot(x,y1,'^r','MarkerFaceColor','none','MarkerEdgeColor','r','LineWidth',1)
hold on
plot(x,y2,'diamondb','MarkerFaceColor','none','MarkerEdgeColor','b','LineWidth',1)
hold on
plot(x,y3,'*k','MarkerFaceColor','none','MarkerEdgeColor','k','LineWidth',1)
hold on
errorbar(x,y1,err,'^r','MarkerFaceColor','none','MarkerEdgeColor','r','LineWidth',0.5)
errorbar(x,y2,err2,'diamondb','MarkerFaceColor','none','MarkerEdgeColor','b','LineWidth',0.5)
errorbar(x,y3,err3,'*k','MarkerFaceColor','none','MarkerEdgeColor','k','LineWidth',0.5)
legend('5vol% DMSO doped ','10vol% DMSO doped ','15vol% DMSO doped ','fontsize',12)
xlim([0 350])
ylim([0 70])
set(gca,'linewidth',1)
ylabel('S (uV/K)','fontsize',14)
xlabel('Bathing Time (min)','fontsize',14)
```

```
%Seebeck coefficient plot for all EG doped samples
x = [0 60 120 180 240 300];
y1 = [33.2 36.5 51.1 46.3 36.7 13.0];
y2 = [15.5 20.1 25.2 41.7 27.1 28.4];
y3 = [20.5 41.2 29.4 16.9 16.5 18.9];
err = [4 4.2 7.1 5.7 8.3 7.4];
err2 = [3 5 4 8 10 7];
err3 = [5 6 4 4 3 6];
plot(x,y1,'or','MarkerFaceColor','none','MarkerEdgeColor','r','LineWidth',1)
hold on
plot(x,y2,'vb','MarkerFaceColor','none','MarkerEdgeColor','b','LineWidth',1)
hold on
plot(x,y3,'sk','MarkerFaceColor','none','MarkerEdgeColor','k','LineWidth',1)
hold on
errorbar(x,y1,err,'or','MarkerFaceColor','none','MarkerEdgeColor','r','LineWidth',0.5)
errorbar(x,y2,err2,'vb','MarkerFaceColor','none','MarkerEdgeColor','b','LineWidth',0.5)
errorbar(x,y3,err3,'sk','MarkerFaceColor','none','MarkerEdgeColor','k','LineWidth',0.5)
legend('5vol% EG doped ','10vol% EG doped ','15vol% EG doped ','fontsize',12)
xlim([0 350])
ylim([0 80])
set(gca,'linewidth',1)
ylabel('S (uV/K)','fontsize',14)
xlabel('Bathing Time (min)','fontsize',14)
```

```
%Power factor plot for all DMSO doped samples
x = [0 60 120 180 240 300];
y1 = [9.49 29.8 80.3 60.7 30.1 18.2];
y2 = [10.8 42.7 68.8 112 122 46.5];
y3 = [8.59 19.1 74.6 51.6 32.3 8];
err = [3.4 11.7 27 24 19.6 6.7];
err2 = [3.1 19.6 27.8 24.3 42.3 26.3];
err3 = [4.2 6.3 29.8 15.4 10.7 3.1];
plot(x,y1,'^r--','MarkerFaceColor','none','MarkerEdgeColor','r','LineWidth',0.7)
hold on
plot(x,y2,'diamondb--','MarkerFaceColor','none','MarkerEdgeColor','b','LineWidth',0.7)
hold on
plot(x,y3,'*k--','MarkerFaceColor','none','MarkerEdgeColor','k','LineWidth',0.7)
hold on
errorbar(x,y1,err,'^r','MarkerFaceColor','none','MarkerEdgeColor','r','LineWidth',0.5)
errorbar(x,y2,err2,'diamondb','MarkerFaceColor','none','MarkerEdgeColor','b','LineWidth',0.5)
errorbar(x,y3,err3,'*k','MarkerFaceColor','none','MarkerEdgeColor','k','LineWidth',0.5)
legend('5vol% DMSO doped ','10vol% DMSO doped ','15vol% DMSO doped ','fontsize',12)
xlim([0 350])
ylim([0 250])
set(gca,'linewidth',1)
ylabel('PF (uW/mK^2)','fontsize',14)
xlabel('Bathing Time (min)','fontsize',14)
```

```
%Power factor plot for all EG doped samples
x = [0 60 120 180 240 300];
y1 = [41.9 116 310 317 192 20.1];
y2 = [13.7 30.1 60.2 230 103 106];
y3 = [18.6 121 71.7 31.1 37.7 45.4];
err = [5.1 19 85 64 43 11.8];
err2 = [7.6 12.6 21.2 57.2 30.2 19.3];
err3 = [5.2 37.2 15.9 18.7 14.6 20.3];
plot(x,y1,'or--','MarkerFaceColor','none','MarkerEdgeColor','r','LineWidth',0.7)
hold on
plot(x,y2,'vb--','MarkerFaceColor','none','MarkerEdgeColor','b','LineWidth',0.7)
hold on
plot(x,y3,'sk--','MarkerFaceColor','none','MarkerEdgeColor','k','LineWidth',0.7)
hold on
errorbar(x,y1,err,'or','MarkerFaceColor','none','MarkerEdgeColor','r','LineWidth',0.5)
errorbar(x,y2,err2,'vb','MarkerFaceColor','none','MarkerEdgeColor','b','LineWidth',0.5)
errorbar(x,y3,err3,'sk','MarkerFaceColor','none','MarkerEdgeColor','k','LineWidth',0.5)
legend('5vol% EG doped ','10vol% EG doped ','15vol% EG doped ','fontsize',12)
xlim([0 380])
ylim([0 600])
set(gca,'linewidth',1)
ylabel('PF (uW/mK^2)','fontsize',14)
xlabel('Bathing Time (min)','fontsize',14)
```

APPENDIX B

SEM RESULTS

Spin coated pristine PEDOT:PSS ~200nm

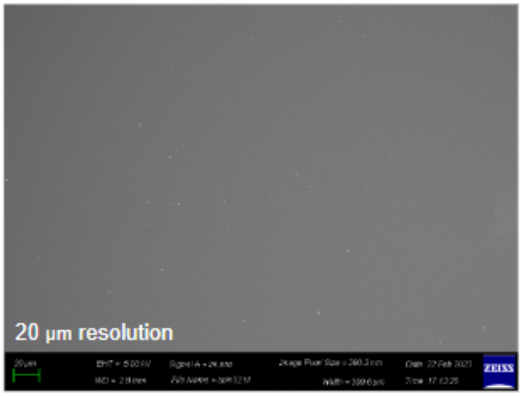

Drop casted pristine PEDOT:PSS ~10um

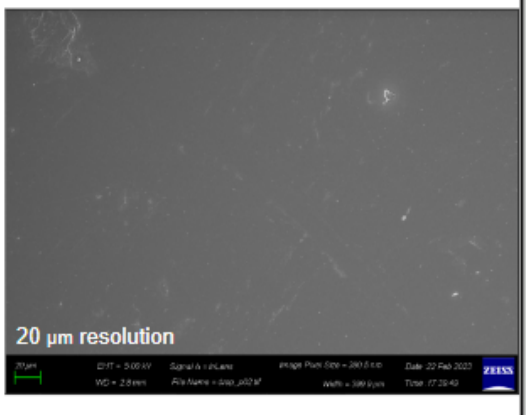

Drop casted pristine PEDOT:PSS

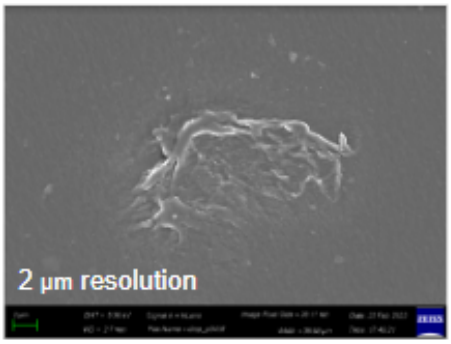

Drop casted PEDOT:PSS After doping(DMSO) and post-treatment(EG)

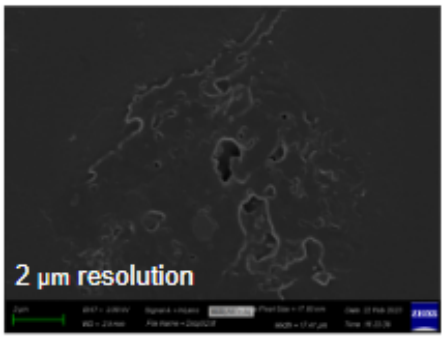

BIBLIOGRAPHY

[1] M. Ge et al., "Experimental study of thermoelectric generator with different numbers of modules for waste heat recovery," Applied Energy, vol. 322, p. 119523, 2022. doi:10.1016/j.apenergy.2022.119523

[2] Y. Zhang and S.-J. Park, "Flexible organic thermoelectric materials and devices for wearable green energy harvesting," Polymers, vol. 11, no. 5, p. 909, 2019. doi:10.3390/polym11050909

[3] O. Bubnova et al., "Optimization of the thermoelectric figure of meritt in the conducting polymer poly(3,4-ethylenedioxythiophene)," Nature Materials, vol. 10, no. 6, pp. 429–433, 2011. doi:10.1038/nmat3012

[4] J. Yang, X. Li, Y. Jia, J. Zhang, and Q. Jiang, "Enhanced Thermoelectric performance of Pedot: PSS Films via Ionic Liquid Post-treatment," Chinese Physics B, vol. 31, no. 2, p. 027302, 2022. doi:10.1088/1674-1056/ac2487

[5] S.-H. Chung, D. H. Kim, H. Kim, H. Kim, and S. W. Jeong, "Thermoelectric properties of PEDOT: PSS and acid-treated SWCNT composite films," Materials Today Communications, vol. 23, p. 100867, 2020. doi:10.1016/j.mtcomm.2019.100867

[6] K. Suemori, S. Hoshino, and T. Kamata, "Flexible and lightweight thermoelectric generators composed of carbon nanotube–polystyrene composites printed on film substrate," Applied Physics Letters, vol. 103, no. 15, 2013.

doi:10.1063/1.4824648

[7] L. Tzounis, "Organic thermoelectrics and thermoelectric generators (tegs)," Advanced Thermoelectric Materials for Energy Harvesting Applications, 2019. doi:10.5772/intechopen.86946

[8] Q. Zhang, Y. Sun, W. Xu, and D. Zhu, "Organic Thermoelectric Materials: Emerging Green Energy Materials converting heat to electricity directly and efficiently," Advanced Materials, vol. 26, no. 40, pp. 6829–6851, 2014. doi:10.1002/adma.201305371

[9] S. Peng et al., "A review on organic polymer-based thermoelectric materials," Journal of Polymers and the Environment, vol. 25, no. 4, pp. 1208–1218, 2016. doi:10.1007/s10924-016-0895-z

[10] J. Li, A. B. Huckleby, and M. Zhang, "Polymer-based thermoelectric materials: A review of Power Factor Improving Strategies," Journal of Materiomics, vol. 8, no. 1, pp. 204–220, 2022. doi:10.1016/j.jmat.2021.03.013

[11] "Thermoelectric properties of bismuth telluride–filled silicone," Nanomaterials for Thermoelectric Devices, pp. 115–126, 2018. doi:10.1201/9780429488726-13

[12] P. K. Sharma, T. D. Senguttuvan, V. K. Sharma, and S. Chaudhary, "Revisiting the thermoelectric properties of lead Telluride," Materials Today Energy, vol. 21, p. 100713, 2021. doi:10.1016/j.mtener.2021.100713

[13] L. Chen, R. Liu, and X. Shi, "Review of Inorganic Thermoelectric Materials," Thermoelectric Materials and Devices, pp. 81–145, 2021. doi:10.1016/b978-0-12-818413-4.00004-1

[14] K. Zhang, Y. Zhang, and S. Wang, "Enhancing thermoelectric properties of organic composites through hierarchical nanostructures," Scientific Reports, vol. 3, no. 1, 2013. doi:10.1038/srep03448

[15] M. R. BHUİYAN, H. MAMUR, M. A. ÜSTÜNER, and Ö. F. DİLMAÇ, "Current and future trend opportunities of thermoelectric generator applications in waste heat recovery," Gazi University Journal of Science, vol. 35, no. 3, pp. 896–915, 2022. doi:10.35378/gujs.934901

[16] "Measuring electrical conductivity: Introduction to continuous analytical measurement: Textbook," Control, https://control.com/textbook/continuous-analytical-measurement/conductivity-measurement

[17] Y. SINGH, "Electrical resistivity measurements: A Review," International Journal of Modern Physics: Conference Series, vol. 22, pp. 745–756, 2013. doi:10.1142/s2010194513010970

[18] B. Russ, A. Glaudell, J. J. Urban, M. L. Chabinyc, and R. A. Segalman, "Organic thermoelectric materials for energy harvesting and temperature control," Nature Reviews Materials, vol. 1, no. 10, 2016. doi:10.1038/natrevmats.2016.50

[19] “Four point probe,” Four point probe - LNF Wiki, https://lnf-wiki.eecs.umich.edu/wiki/Four-point-probe

[20] “Four-point probe manual,” Four Point Probes, https://four-point-probes.com/four-point-probe-manual

[21] J. de Boor and E. Müller, “Data Analysis for Seebeck coefficient measurements,” Review of Scientific Instruments, vol. 84, no. 6, p. 065102, 2013. doi:10.1063/1.4807697

[22] A. T. Burkov, A. Heinrich, P. P. Konstantinov, T. Nakama, and K. Yagasaki, “Experimental set-up for thermopower and resistivity measurements at 100-1300 K,” Measurement Science and Technology, vol. 12, no. 3, pp. 264–272, 2001. doi:10.1088/0957-0233/12/3/304

[23] B. Dörling, O. Zapata-Arteaga, and M. Campoy-Quiles, “A setup to measure the Seebeck coefficient and electrical conductivity of anisotropic thin-films on a single sample,” Review of Scientific Instruments, vol. 91, no. 10, p. 105111, 2020. doi:10.1063/5.0021715

[24] “Spin coating,” Spin Coating - an overview — ScienceDirect Topics, https://www.sciencedirect.com/topics/materials-science/spin-coating

[25] A. Kaliyaraj Selva Kumar, Y. Zhang, D. Li, and R. G. Compton, “A mini-review: How reliable is the drop casting technique?,” Electrochemistry Communications, vol. 121, p. 106867, 2020. doi:10.1016/j.elecom.2020.106867

[26] T.-R. Chou et al., "Highly conductive pedot:PSS film by doping P-toluenesulfonic acid and post-treatment with dimethyl sulfoxide for ITO-free polymer dispersed liquid crystal device," Organic Electronics, vol. 48, pp. 223–229, 2017. doi:10.1016/j.orgel.2017.05.052

[27] A. T. Burkov, A. Heinrich, P. P. Konstantinov, T. Nakama, and K. Yagasaki, "Experimental set-up for thermopower and resistivity measurements at 100-1300 K," Measurement Science and Technology, vol. 12, no. 3, pp. 264–272, 2001. doi:10.1088/0957-0233/12/3/304

[28] A. Guan et al., "An experimental apparatus for simultaneously measuring Seebeck coefficient and electrical resistivity from 100 K to 600 K," Review of Scientific Instruments, vol. 84, no. 4, p. 043903, 2013. doi:10.1063/1.4798647